iScience

Article

Development of a mussel-inspired conductive graphene coated cotton yarn for wearable sensors

Graphical abstract

Highlights

- Cotton yarn modified with PDA enhances graphene's absorption properties
- A simple dip-coating method improves conductivity over the conventional curing process
- Sensors with low resistance, high sensitivity, and durability was made for wearables

Authors

Guanliang He, Chuang Zhu, Yuze Shi, ..., Constantinos Soutis, Le Cao, Xuqing Liu

Correspondence

chuang.zhu@dhu.edu.cn (C.Z.), caole@xust.edu.cn (L.C.), xqliu@nwpu.edu.cn (X.L.)

In brief

Natural sciences; Applied sciences; Materials science

He et al., 2025, iScience *28*, 111711
February 21, 2025
https://doi.org/10.1016/j.isci.2024.111711

CellPress

iScience

CellPress
OPEN ACCESS

Article

Development of a mussel-inspired conductive graphene coated cotton yarn for wearable sensors

Guanliang He,[1,2] Chuang Zhu,[3,*] Yuze Shi,[1] Yingjia Yu,[1] Yi Wu,[1] Constantinos Soutis,[2] Le Cao,[4,*] and Xuqing Liu[1,5,6,*]
[1]Shandong Laboratory of Advanced Materials and Green Manufacturing at Yantai, Yantai, Shandong 264006, China
[2]Department of Materials, School of Natural Sciences, University of Manchester, Oxford Rd, Manchester M13 9PL, UK
[3]Key Laboratory of Textile Science & Technology, Ministry of Education, College of Textiles, Donghua University, Shanghai 201620, China
[4]School of Electric and Control Engineering, Xi'an University of Science and Technology, Xi'an 710054, China
[5]State Key Laboratory of Solidification Processing, Center of Advanced Lubrication and Seal Materials, School of Materials Science and Engineering, Northwestern Polytechnical University, Xi'an, Shanxi 710072, China
[6]Lead contact
*Correspondence: chuang.zhu@dhu.edu.cn (C.Z.), caole@xust.edu.cn (L.C.), xqliu@nwpu.edu.cn (X.L.)
https://doi.org/10.1016/j.isci.2024.111711

SUMMARY

Graphene-based flexible yarn sensors are promising due to their exceptional conductivity and user-friendly properties, but ensuring stable graphene adsorption on fibers for long-term durability remains challenging. Herein, we produce a flexible polydopamine (PDA)-modified cotton yarn via a simple dip-coating process using a self-made sodium deoxycholate (SDC)-modified graphene dispersion, avoiding non-biodegradable, corrosion-prone metallic coatings. The resulting sensor exhibits low electrical resistance (as low as 21.1Ω ± 0.2/cm), high bending sensitivity (resistance change rate of 3.557 ± 0.002 for bending ranges from 40% to 100%), and outstanding durability over 2,000 flexural bending cycles. It can monitor various human body movements and physiological states and be integrated into wearable electronic textiles (e-textiles) for applications like monitoring knee movements, recognizing hand gestures, and detecting thoracic respiratory status. This work highlights the sensor's potential in personal and public healthcare applications.

INTRODUCTION

Flexible strain sensors are a crucial component in wearable electronic textiles. The market for electronic textiles, propelled by integrating lightweight and flexible electronics into everyday clothing, is projected to reach $5 billion by 2027.[1] The flexibility, breathability, and significant potential of these textiles in areas like continuous human-computer interaction and health monitoring have attracted extensive research interest.[2–4] Due to their uncomplicated manufacturing process, cost-effectiveness, and high sensitivity, recent studies have primarily concentrated on resistance-based strain sensors.[5] Nonetheless, significant challenges persist, particularly regarding the complex thermal sintering production process and the employment of non-biodegradable, corrosion-prone metallic materials.[6,7] Previous research reported that silver (Ag) has been coated on diverse fibers, including polyethylene terephthalate (PET), aramid, glass, cotton, and polyurethane, through PDA-assisted electroless plating (ELD).[8–10] However, these metals are relatively rigid, and not bendable.[11] While newer materials such as carbon nanotubes (CNTs), carbon black, and graphene have been developed,[12] their limited inherent adhesion to substrates due to chemical inertness,[13] lead to a weak adhesive bond between the conductive network and the textile-based substrate. Thus, they are prone to separation under repeated deformation, which results in a decline in both mechanical and electromagnetic performance. According to Lee's research,[14] dopamine, emulating mussel adhesion chemistry, promotes the spontaneous formation of nanoscale polydopamine (PDA) films, which attach to virtually all material surfaces, including polymers, ceramics, semiconductors, and 2D metals, through a simple immersion in an alkaline solution.

Recent work indicated that the remarkable absorption capability of dopamine has led to the modification of a variety of substrates, including graphene oxide and electrospun nanofibers. Some reports have also shown the simultaneous reduction for functional graphene oxide using dopamine derivatives.[15] Xie develop a dopamine-based nanocomposite hydrogel sensor comprising polyacrylic acid (PAA) and reduced graphene oxide (rGO).[16] However, the presence of oxygen-containing groups in graphene oxide disrupts its structure, significantly diminishing its electrochemical performance.[17,18] In practical applications, issues such as energy dissipation, heat generation, and unstable conductivity due to high resistance can compromise the user experience of e-textiles.

Herein, a technique using a micro-fluidic device to cyclically exfoliate graphite, dispersing them through sodium deoxycholate (SDC) modification. Contrary to the majority of studies employing organic solvents for graphene solutions, PDA substantially

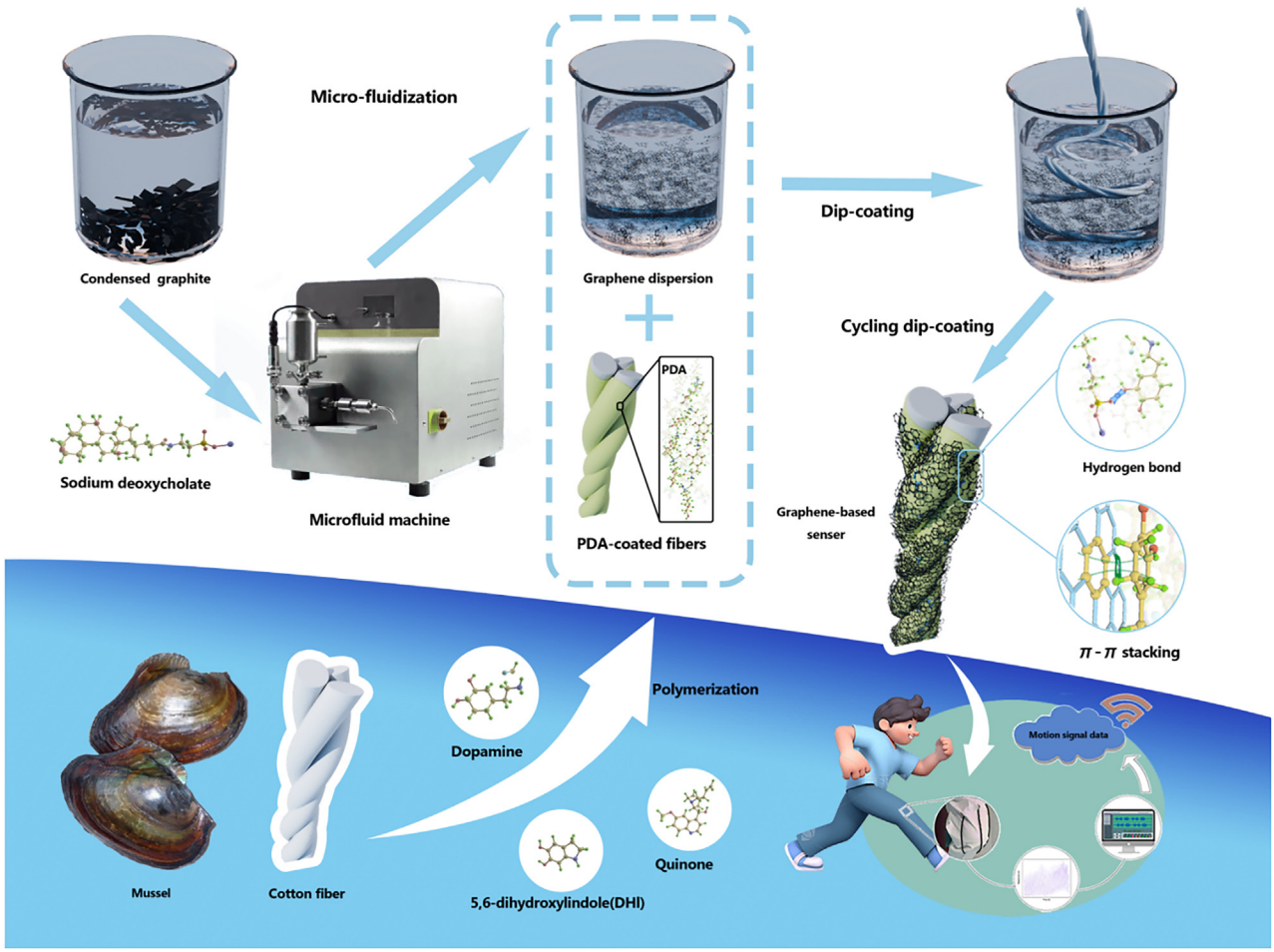

Figure 1. A schematic illustrating the production of graphene sensors based on polydopamine (PDA) and their integration in e-textiles for healthcare monitoring

enhances the adhesion of graphene coatings to fiber surfaces via chemical interactions with graphene platelets/SDC by hydrogen bond and π–π bond.[19] This method leads to the self-assembling of PDA coatings onto fiber surfaces, thereby facilitating the fabrication of flexible sensors, as depicted in Figure 1. The manufacturing processes for graphene and sensors were simplified, employing a straightforward cyclical dip-coating and air-drying method, resulting in enhanced electrical conductivity. Furthermore, these sensors have been integrated into clothing to detect movements in the knee, finger joints, and thorax during typical human activities, yielding stable electrical signals via resistance changes (ΔR/R), and demonstrating significant potential in applications such as motion detection, human-computer interaction, and respiratory health monitoring.

RESULTS AND DISCUSSION

Characterization of graphene dispersion and graphene-based sensor yarn

The lateral dimensions and thickness of the exfoliated graphene plates were determined using scanning electron microscopy (SEM) and atomic force microscopy (AFM). Droplets of graphene dispersion were placed onto silicon wafers and subsequently dried during the heating stage (in air and N_2 gas atmosphere). The morphology of the graphene was examined under a magnification of 10,000 times. The morphology and lateral size of the graphite is illustrated by Figure S1. Subsequently, hundreds of graphene plates were randomly selected for statistical analysis of their lateral dimensions and thickness.

As Figure 2A displays, the morphology of the graphene after 100 cycles was exfoliated and fragmented. The lateral size of graphene following 75/100/125 cycles were statistically analyzed using SEM, as shown in Figure 2B. As the number of cycles increased, the distribution of graphene lateral size shifted leftward, resulting in a decrease in the average graphene lateral size. The lateral size of the graphene produced in this study predominantly fell within the 0.5–1.5 mm range. This range is deemed ideal for the lateral size of graphene.[20] Any smaller lateral size of graphene impacts on the specific surface area that diminishes the sensitivity of the sensor. Excessively large lateral sizes could adversely affect the mechanical properties of the sensor.[21,22] Therefore 120 cycles of microfluidization did

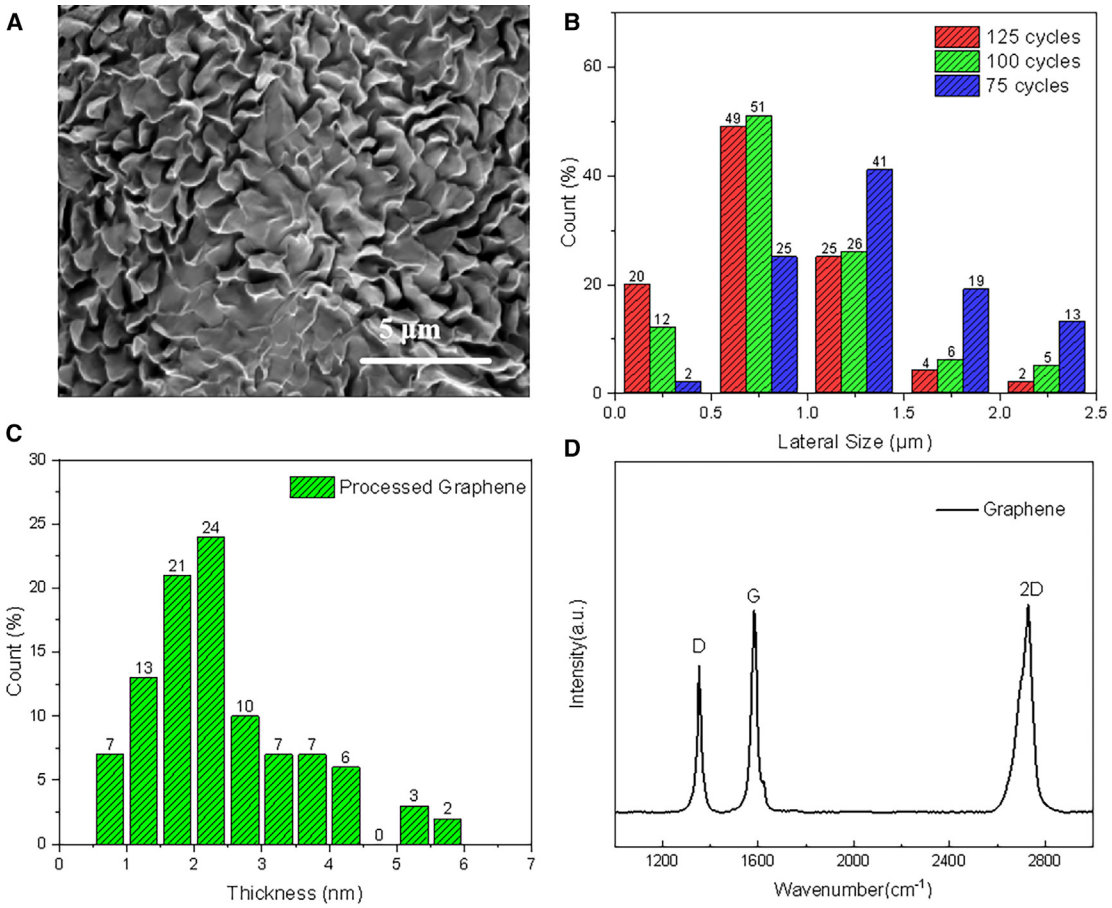

Figure 2. Characterization of graphene dispersion

(A) Morphology of graphene flakes.

(B) Graphene lateral size under different cycles of microfluidization.

(C) Thickness distribution of graphene.

(D) Graphene Raman spectrum.

not result in significant improvement in the quality of graphene. 70 cycles of micro-fluidization did not meet the required average lateral sizes. Therefore, 100 cycles were determined to be the optimal method for preparing graphene.

The thickness distribution following 100 cycles was determined using AFM, as depicted in Figure 2C. The AFM scanned an area of approximately 20 μm × 20 μm on the substrate, measuring 100 plates under each treatment condition. Statistical analysis revealed that most samples were concentrated between 1 and 2.5 nm. The AFM imagine is shown in Figure S2. These data are consistent with other studies on the preparation of high-performance graphene.[23] The average thickness of the graphene prepared by this method was found to be 1.93 nm. The Raman spectrum of the samples containing graphene was shown in Figure 2D. The method of sample preparation was the same as that used for SEM analysis. The Raman spectrum of graphene exhibited characteristic peaks at approximately 1,352.05 cm^{-1}, 1,582.53 cm^{-1}, and 2,727.99 cm^{-1}, corresponding to the D, G, and 2D bands, observable in all samples. The D/G to 2D height ratio was approximately 1:1, indicating that the graphene consisted of single or few layers. The D band suggested a small degree of defects in graphene, attributed to edge effects and structural defects introduced during the micro-fluidization process that could affect conductivity.

For the preparation of graphene-based sensors, PDA was synthesized on cotton fiber surfaces via pH-induced polymerization. This PDA demonstrated robust surface adhesion properties, offering a platform for subsequent adsorption. Fourier transform infrared spectroscopy (FTIR) was employed to confirm the successful deposition of PDA. As indicated in Figure 3A comparative analysis was conducted between untreated pure cotton fibers and those modified with PDA. An observed peak at 1,612 cm^{-1}, corresponding to the N–H bending vibrations of amine groups in PDA, confirmed the successful PDA coating on the cotton fibers. To elucidate the chemical bonding between PDA and graphene dispersions, the nano-powders on the sensor surfaces were scraped off, compressed into pellets and tested by x-ray photoelectron spectroscopy (XPS). The C 1s (as presented in Figure 3B) of G-SDC-PDA cotton fiber sample spectrum exhibited four peaks: C–O at 285.3 eV, characteristic of

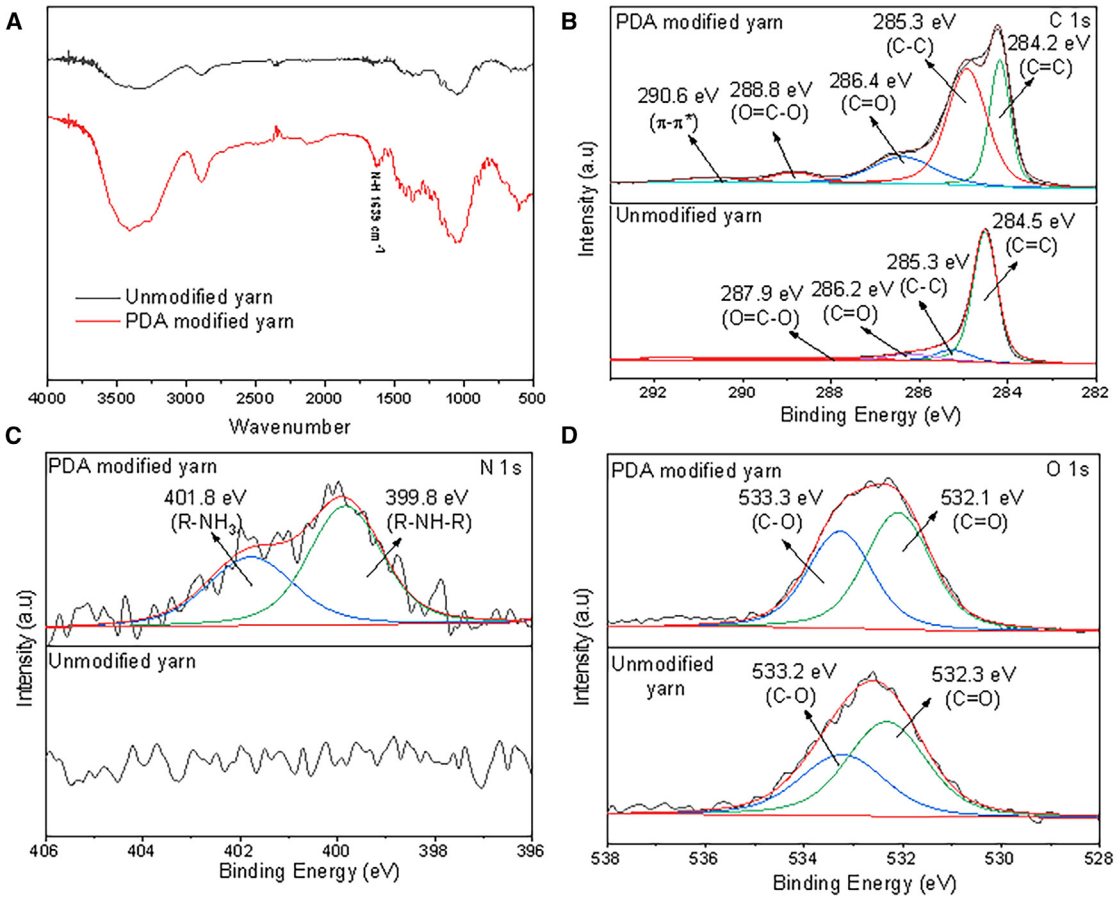

Figure 3. Characterization of PDA modified yarn

(A) FTIR spectrum of the modified/unmodified sample.

(B) XPS spectra of the PDA modified/unmodified sample with C 1s.

(C) XPS spectra of the PDA modified/unmodified sample with N 1s.

(D) XPS spectra of the PDA modified/unmodified sample with O 1s.

the PDA layer; C=C sp^2 at 284.2 eV, indicative of graphene; O–C=O at 288.8 eV, derived from a minor component of cotton fiber cellulose; and a satellite peak (π-π). π-π stacking, a van der Waals force related to the π-electron skeletal system of molecules, is critical for forming stable hybrid structures. Cotton fiber cellulose, composed of aromatic molecules, effectively engages in intermolecular π-π stacking during self-assembly.[24] This π–π stacking between the graphene surface and aromatic molecules typically renders the surface assembly stable during washing or other solution treatments. Notably, PDA treatment enhanced the surface activity of the cotton fibers, thereby increasing their interfacial adhesive strength. Importantly, comparing the XPS spectra of unmodified samples, the change of C 1s (284.2) binding energy is lower than that of C 1s (284.5 eV) of unmodified yarn, indicating potential hydrogen-bonding interaction with graphene/SDC plates. The N 1s energy level spectrum (shown in Figure 3C) displayed a peak at 401.8 eV, attributed to primary amine (R–NH_3) components, was compared with the spectra of unmodified yarn samples that exhibited no peak, suggesting the graphene successfully adhered to the PDA-coated fibers. Another peak at 399.8 eV, linked to secondary amine components (–R–NH–R), reflecting the interaction between PDA and accepted intermediates. Figure 3D illustrates the spectrum of O 1s. The spectra of modified yarn present two peaks at 532.3 eV and 533.2 eV, assigned to C–O and C=O groups from SDC and PDA, respectively. The O 1s spectral energy levels of unmodified yarn has no obvious change compared with modified yarn, which indicates the epoxy group does not participate in adsorption.

Electrical conductivity is crucial for wearable e-textiles. To enhance the conductivity of sensors and demonstrate the graphene flake adsorption efficiency of PDA-coated cotton, both unmodified and PDA-modified cotton yarns were immersed into the graphene solution for dip-coating. This process was repeated until the sensors reached adsorption saturation, allowing graphene to adhere to the substrate, as depicted in Figure 4A. Compared to unmodified cotton yarns, those with PDA coating exhibited a darker color, indicating more substantial graphene adsorption. In contrast, the uncoated yarns showed minimal graphene flake adsorption without a continuous graphene layer.

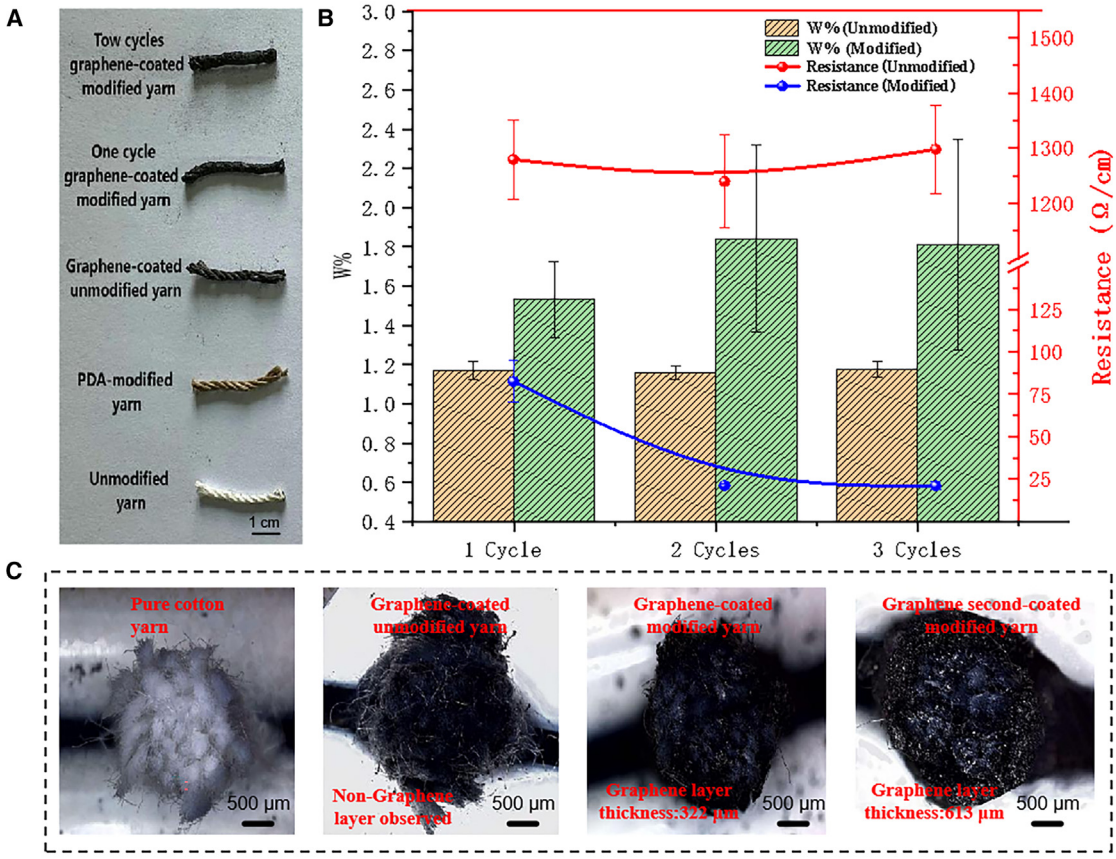

Figure 4. Characterization of graphene-coated yarn sensors

(A) Photographs of various samples.

(B) A corresponding graph showing the relationship between the graphene weight percentage (w%) and the electrical resistance of each sample. Data are represented as mean ± SEM. (n = 3).

(C) The optical microscope images of the cross-sections.

After two coating cycles, the yarns adsorbed more graphene, resulting in complete, thicker coatings.

As Figure 4B illustrates the relationship between the graphene adsorption content by weight, W%, and the electrical resistance (Ω/cm) of each sample; the adsorption quantity W% is defined as: W% = (W + Wi)/W, where W is the initial weight of the cotton fabric, and Wi is the weight increment after each dip-coating process. The untreated yarn samples exhibited high and unstable electrical resistance, up to 1.27 KΩ/cm. Moreover, after subjecting the untreated yarns to multiple dip-coating cycles, it was exhibited that their w% reached and plateau, and there was no significant reduction in resistance. This was potentially due to the untreated yarns reaching their saturation capacity for graphene absorption during the first cycle. However, the resistance of PDA-treated yarns reduced significantly to 82.5 Ω/cm after one dip-coating, demonstrating high electrical conductivity due to the strong graphene adsorption capability of PDA-coated cotton yarns. The resistance reached its lowest point of 21.1 Ω/cm after the second cycle and remained stable through subsequent treatments. The W% data also indicated that the yarns' adsorption capacity for graphene approached saturation after the second cycle and remained largely unchanged thereafter. Consequently, a two-cycle dip-coating process can be considered as the standard protocol for producing sensor samples. Figure 4C illustrates the respective cross-sectional views of the samples obtained by depth of field optical microscopy with no graphene layer observed in the uncoated yarn. In contrast, the modified-yarn coated twice, displayed a significantly thicker outer graphene layer, with an approximate thickness of 613 μm, marking a considerable increase from the 193 μm noted in the single-coated yarn, which suggests that graphene can accumulate through van der Waals forces.[25] After a graphene layer is adsorbed on the yarn, subsequent coatings lead to further accumulation of graphene flakes through van der Waals forces, markedly improving the yarn's electrical properties.

It is interesting to note that in comparison with previous reports,[26] graphene sensors adopt a complex thermal sintering manufacturing process to ensure the water evaporation. In this study, the curing process was repeated (refer to Figure S3). However, the resistance in sensors prepared through thermal sintering exceeded that of sensors produced by the direct air-drying process. It is hypothesized that the elevated temperatures led to the decomposition of SDC,[27] adversely affecting its ability to modify graphene. This presumably weakened the

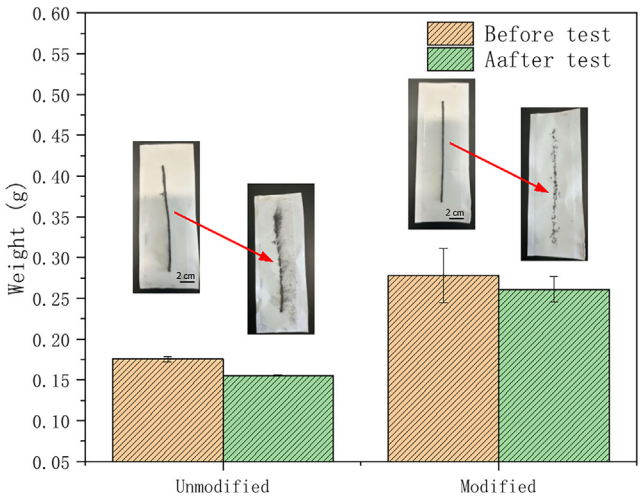

Figure 5. Mechanical delamination experiments on graphene sensors under harsh conditions

Data are represented as mean ± SEM. (n = 3).

adhesion of graphene to the fiber surface, thereby resulting in increased electrical resistance. To further explore the capability of graphene adsorption by PDA-modified yarn, the harsh environment test was applied. The modified graphene yarn and unmodified graphene yarn were used for comparison, fixed with 3M adhesive tape, and subjected to a force of 0.98 ± 0.02 N on each type of yarn. Afterward, the yarns were placed in an ultraviolet chamber to simulate harsh environment condition (65 ± 2°C) for 2 h (as shown in Figure S4). Subsequently, the tested yarns were peeled off, and the weight of the different yarns before and after the experiment was recorded and compared to indicate the amount of graphene peeled off during the test.

Figure 5 shows the weight reduction of both modified and unmodified yarns under harsh environment test due to the peeling off of graphene before and after the tests. The average w% reduction of the modified yarn after the experiment is 6.2%, and the average w% reduction of the unmodified yarn is 11.4%, which indicates that the PDA-modified yarn still has good graphene adsorption capability after experiencing harsh external environments. The photos above the bar chart display the graphene yarns before the test and the residues on the tape after the graphene was peeled off following the test. Comparing the graphene remain in Figure 5, it is evident that most of the graphene was peeled off from the unmodified yarn and remained on the tape, whereas less amount of graphene was peeled from the modified graphene yarn and left on the tape. Considering that the modified yarns adsorbed more graphene, this experimental data demonstrates the effectiveness of PDA-modified yarns in graphene adhesion.

The volume of adsorption and the distribution of graphene are crucial factors influencing the electrical properties of conductive fibers. Observations via SEM have shown that the cotton yarn modified with PDA exhibits a substantial increase in its capacity to adsorb graphene. To analyze the enhanced adsorption of the yarn following PDA modification, various samples were prepared: an unmodified yarn and two PDA-modified yarns were simultaneously immersed in graphene dispersion for 1 min, then naturally dried in a ventilated cabinet for 24 h. The process was repeated on one of the PDA-modified yarns, yielding four distinct samples: pure cotton yarn, graphene-coated cotton yarn without modification, PDA-modified yarn coated with graphene dispersion, and PDA-modified yarn re-coated with graphene dispersion.

Figures 6A and 6B illustrate the transverse-section and individual fibers of the cotton yarn, respectively. The yarn's surface appeared smooth without noticeable contaminants after undergoing pretreatment processes like desizing and ultraviolet treatment. Figures 6C and 6D show the graphene adsorption of the unmodified cotton yarn, demonstrating sparse graphene flakes on the yarn's transverse-section and limited penetration into the inner layers; there were large bare areas, with a sparse distribution of graphene on the fibers. This corresponds with Figure 4's representation of the unmodified yarn, in which limited external graphene pathways result in reduced conductivity and increased variability.

Conversely, Figures 7A and 7B present the PDA-modified yarn, exhibiting a significant increase in the adsorbed graphene layers, extending to the yarn's core. The yarn's individual fibers were nearly completely coated in graphene, leaving minimal bare areas. Figures 7C and 7D compare samples with two coatings to those in Figures 7A and 7B, revealing a more substantial accumulation of graphene on the yarn, creating continuous graphene bands and markedly enhancing conductivity. The graphene complete coverage on individual fibers, with no visible bare areas, indicates the full realization of the cotton yarn's graphene adsorption capacity. Additionally, to examine the uniformity of graphene distribution on the yarn, a 3D optical profilometer was used to measure its surface roughness (as illustrated in Figure S5), with and without the tension controller. The roughness is represented by Sa (arithmetical mean height of the surface).

$$Sa = \frac{1}{A}\iint_{A}\left|z(x,y)\right|dxdy$$

where A is the total area of the surface being measured; z(x,y) is the height of the surface at any point with coordinates; and dxdy is the infinitesimal elements of the surface area over which the integration is performed.

When the tension controller was used, the average Sa is 96,921.152 nm, which is lower than the average Sa of 113,994.96 nm for the graphene-coated yarn without this equipment. Additionally, observations from the 3D optical profilometer imaging reveal irregular graphene distribution and bulging in the yarn, as seen in Figures S6A and S6B. In contrast, Figures S6C and S6D show a uniform distribution of graphene on the yarn, further confirming that the tension controller significantly aids in achieving a more even graphene coating on the yarn during the dip-coating process, confirming that our dip-coating methods effectively ensures a uniform graphene coating. The energy dispersive spectrometer (EDS) image of graphene-coated fiber was present by Figure S7. A notable observation

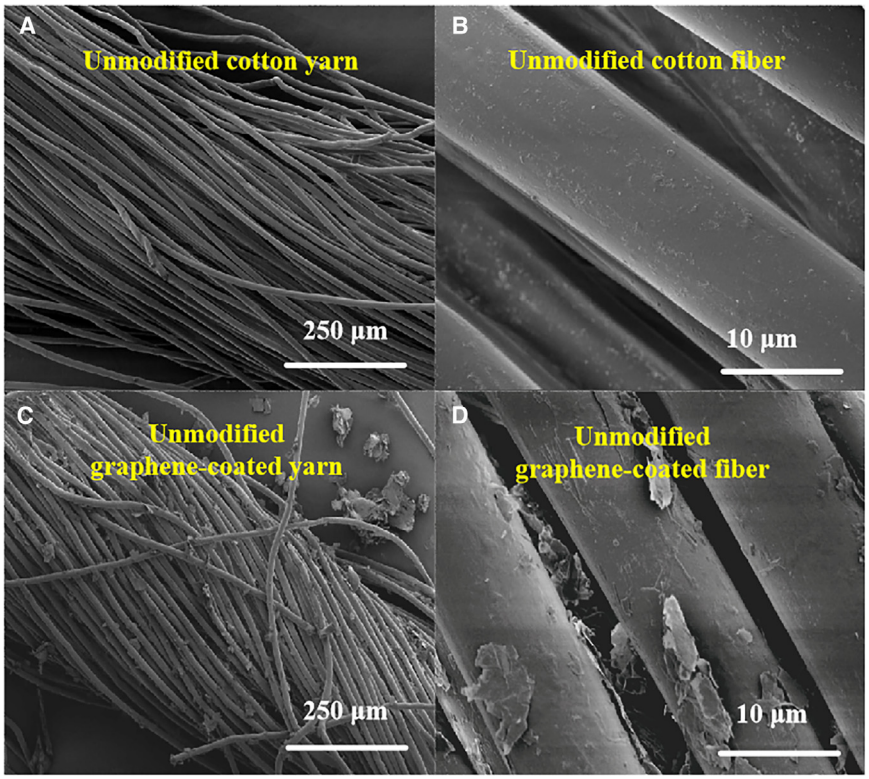

Figure 6. SEM images comparing the transverse-section and the individual fibers morphology

(A) Pure cotton yarn.
(B) Pure cotton fiber.
(C) Unmodified yarn dip-coated with graphene.
(D) Unmodified fiber dip-coated with graphene.

is that Na elements were also detected on the surface of the sample, which is attributed to the residual carried by the SDC remaining on the graphene.

Sensing capability/electro-mechanical characterization of graphene based sensor yarn

Due to the exceptional softness and electrical conductivity of graphene sensors, our study conducted electric-mechanical test on a 10 cm long PDA-modified graphene cotton yarn sensor that had undergone two dip-coating cycles, using a tensile testing machine. The resistance was measured by the KEITHLEY 2611B Source Measure Units. The resistance curves of sample within a 6cm gauge length during the processes of bending and bending back were continuously monitored and recorded. Here, ''gauge length'' refers to the distance between the grips of the tensile tester (as shown in Figure S8). A decrease in gauge length causes the sensor to bend, whereas an increase results in its straightening. The displacement rate was set at 2 mm/s.

Figure 8A illustrates the resistance changes (ΔR/R) of the sensor yarn throughout 5,000s of bending-releasing. After an initial period of 1,500 s, the sensor yarn's resistance change (ΔR/R) is significantly stabilized. During both bending and bending back phases, the yarn demonstrated linear resistance changes. Notably, the adhesion of the graphene coating performed well, with no instances of material detachment and creases on yarn surface observed after 1,000 s. As depicted in Figure 8B, the sensor exhibited resistance changes at varying gauge lengths. Upon reaching a steady state (test duration exceeding 1,500 s), the average ΔR/R for each 10 mm segment during the cyclic test was calculated and presents. Remarkably, the sensor demonstrated a high sensitivity, with a rate of resistance change ($R^* = (\Delta R/R)/\varepsilon$) of 4.58, where R^* is the rate of resistance change, the ΔR represents the change in resistance, R is the initial resistance, ε is the mechanical strain within the gauge length. It exceeded the value of 2.25 reported for an existing graphene textile sensor.[28] It is noteworthy that as the gauge length of the sensor decreased from 100 mm to 90 mm, the rate of resistance change for the bending and bending back processes were 15.1 and 11.6, respectively. This indicates that our graphene sensor exhibits exceptional sensitivity to the initial stages of bending deformation. Therefore, monitoring applications with minimal bending, such as in respiratory monitoring, is possible with the proposed graphene sensor. The linear and stable resistance response to bending test suggests the sensor's potential applicability in wearable and flexible electronics. Figures 8C and 8D illustrate the sensor's capability to detect tensile forces and compression forces. This test is a one-time, irreversible procedure for each graphene sensor. Once the testing is completed, the sensor's electrical resistance cannot return to its initial level of conductivity. During the tensile test, both ends of the sample were secured by clamps and extend upward at a rate of 1 mm per second. The test was halted once the tensile force reached 20% of its peak value. In this context, the blue line denotes the variation in resistance, and the red line indicates the changes in tensile force. The yarn maintained elastic behavior up to 1% strain, with resistance increasing linearly with tensile force. At 1% strain, the material's maximum stress point, cracks were observed in the graphene outer layer, leading to a sharp rise in resistance. Beyond 1.5% strain, the resistance escalated beyond the measurable range, indicating that the sensor, due to permanent damage to the graphene coating. The gauge factor ($GF = (\Delta R/R)/\varepsilon$, where ε is the mechanical strain experienced) of our graphene sensor reached a value of 266.7. Figure 8D illustrates the resistance change curve of the sensor in a 1 cm × 1 cm lateral compression test. Initially, the resistance decreases within a 15 ± 0.2 N force range as the graphene flakes compact under compressive applied load. However, beyond this load level, the resistance begins to increase, attributable to damage to the graphene coating, and eventually peaks at 77.5 ± 0.2 N. During the compression test,

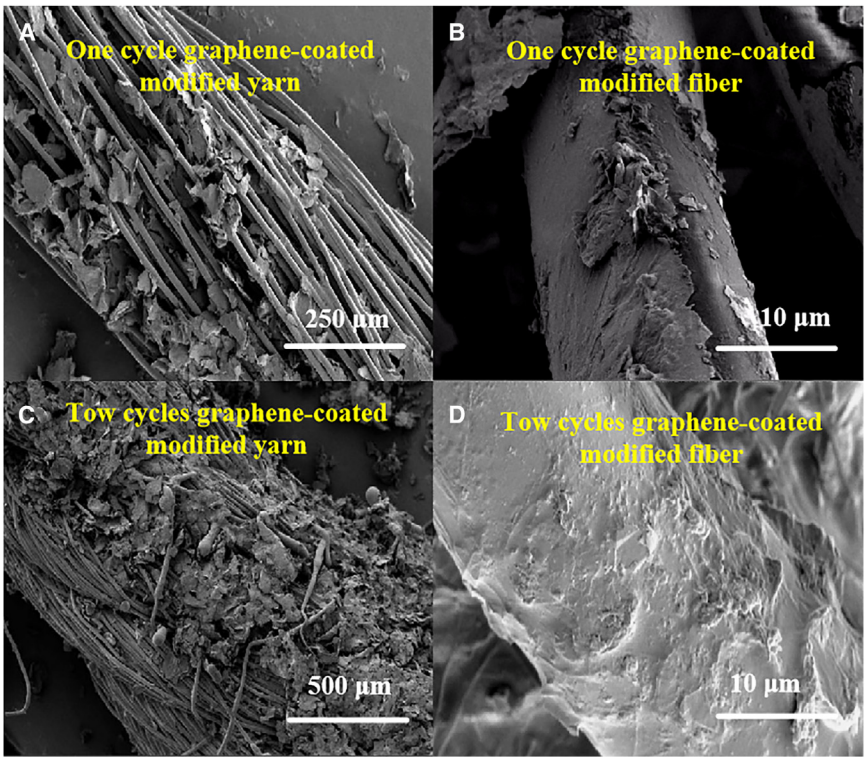

Figure 7. SEM images comparing the transverse-section and the individual fibers morphology

(A) Yarn modified with PDA and dip-coated with graphene.

(B) Fiber modified with PDA and dip-coated with graphene.

(C) PDA-modified yarn re-dip-coated with graphene.

(D) PDA-modified fiber re-dip-coated with graphene.

the sensor exhibits a non-linear response. As previous studies indicated that when graphene coatings are compressed with a roller, their resistance decreases.[29] This is attributed to the pressure compacting the graphene layers, thereby enlarging the area of contact between them, which in turn facilitates more extensive conduction pathways (refer to Figure S9). Nonetheless, following the pressure testing, the appearance of cracks was noted on the sensor's coating. This suggests that the sustained escalation of pressure compromises the structural integrity of the graphene coating, leading to an increase in electrical resistance.

Applications of wearable sensors in monitoring fields

Considering the exceptional sensitivity, durability, and electrical conductivity of the graphene-based PDA-coated cotton yarn sensors, we have advanced the demonstration of their performance across various body movements. Three sensors, each measuring 10 cm long, were initially attached to the knee region of a participant. These sensors were secured to the skin using medical adhesive tapes, and boast an ultra-lightweight and highly flexible design, thereby ensuring minimal interference with the natural range of motion. This setup is detailed in Figures 9A–9D, serving to validate their effectiveness as motion monitoring sensors across diverse activities, including walking, cycling, jogging, and jumping.

As depicted in Figures 9A–9D, the resistance signals align consistently with the variation in knee angles across different movement states. The variance resistance of individual knee sensors is very small and the convergence of their resistance profiles underscores the sensors' high reliability and stability in monitoring knee movements. This is attributed to the reduction in the gap between graphene flakes upon bending, which enlarges the overlap area, thereby enhancing the electrical conductivity and reducing resistance. By analyzing the sensor signals' frequency and amplitude, the subject's movement state can be accurately assessed. This methodology offers significant potential for applications such as optimizing movement strategies for athletes like football players through the collection and analysis of their motion data.

Extending the scope of applications, the integration of sensors on the hands of a human facilitated precise detection of resistance variations during different states (as depicted in Figure 9E), such as releasing, grasping, and holding, which correspond to various hand gestures and positions. This also demonstrates their potential usage in controlling robotic arms.

Breathing, a crucial physiological signal, is effectively captured by the graphene sensor, even for subtle variations. Positioned beneath the chest and secured with an elastic band, the sensor proficiently monitored diverse breathing patterns. The experimental findings, illustrated in Figure 9F, offer distinct evaluations of both the rate and depth of breathing, distinctly differentiating between resting and post-exercise breathing patterns. Importantly, the graphene sensor's heightened sensitivity to minimal initial changes enables the accurate detection of even faint resting breaths. Consequently, these sensors hold promise as early warning systems for conditions such as sudden infant death syndrome and adult sleep apnea (but areas that require further investigation), highlighting the broad applicability and efficacy of graphene-based electronic textiles in a myriad of monitoring contexts. Further development of the sensor and clinical studies will be required in the near future to gain more confidence in its robustness and reliability.

Conclusions

In summary, this study proposes an innovative method to manufacture electrically conductive graphene coated cotton yarns for a wearable sensor. These yarns are flexible, durable (2,000 cycles), possess a high GF (with an electric GF of 3.557 for strain range measurements from 40% to 100%), and exhibit excellent electrical conductivity (21.1 $\pm$ 0.2 Ω/cm resistance). The process (inspired by the composition of adhesive proteins in mussels)

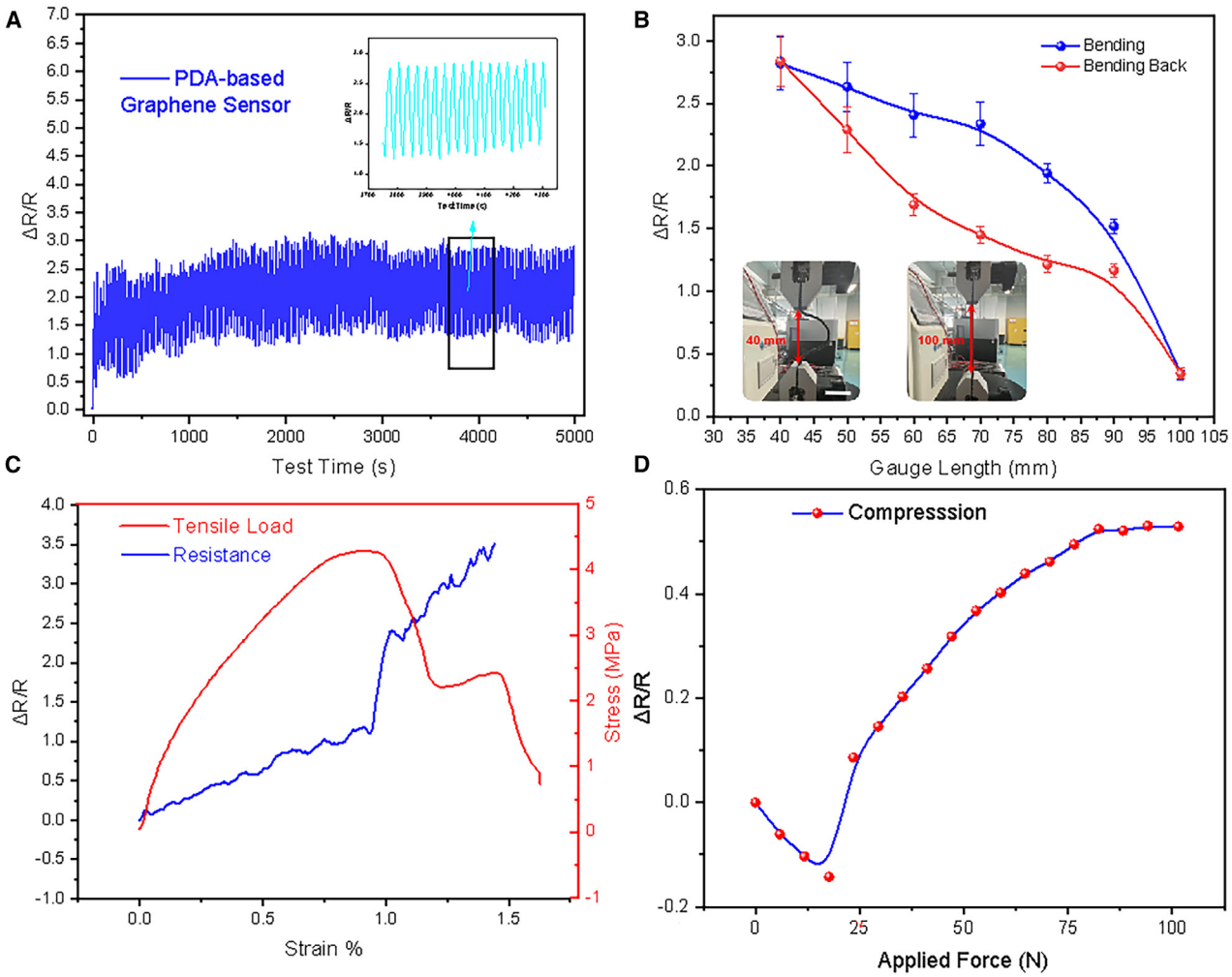

Figure 8. Sensing characteristics of the graphene coated cotton yarns

(A) Cycle bending test.

(B) Bending test. Data are represented as mean ± SEM. (n = 100). The scale bar indicate 2cm.

(C) Tensile test.

(D) Lateral compression test.

starts by immersing the yarn in an alkaline aqueous solution to coat its surface with a PDA nanofilm. PDA modifies the cotton yarn, facilitating its combination with graphene/SDC via hydrogen and π–π bonding, thus enhancing its graphene flake adsorption capacity. Compared to unmodified yarns, PDA-modified sensor yarns present lower electrical resistance, higher adsorption w%, and maintain excellent electrical stability even after many cyclic bending tests. These conductive yarns can be attached to the body using a medical adhesive tape (like a plaster) or embedded in wearable e-textiles as strain-stress sensors to monitor body movement, like knee and finger joints, and could also be applied for human respiratory detection. This could have great potential in sports movement detection of professional athletes, human-computer interaction in robotics and medical care of patients with respiratory system diseases, among many other applications.

Limitations of the study

In this study, an electrically conductive graphene-coated cotton yarns were developed through a PDA modification process and subsequent dip-coating in a graphene dispersion. The resulting yarns exhibited significant enhancements in conductivity, sensitivity, and durability. However several limitations need to be addressed. Firstly, the drying process of the graphene-coated yarns can lead to inconsistencies in the coating thickness, affecting the uniformity of electrical properties across different samples. Secondly, the tensile sensitivity of the sensors cannot be repeatedly used, and the lateral compression test indicate that the resistance changes of the sensors are not liner, which limiting their application in scenarios requiring repeatable and high precision. Finally, the environmental impact of the materials, including the moisture and effects of sweating to the sensors, needs to be considered and mitigated in future research.

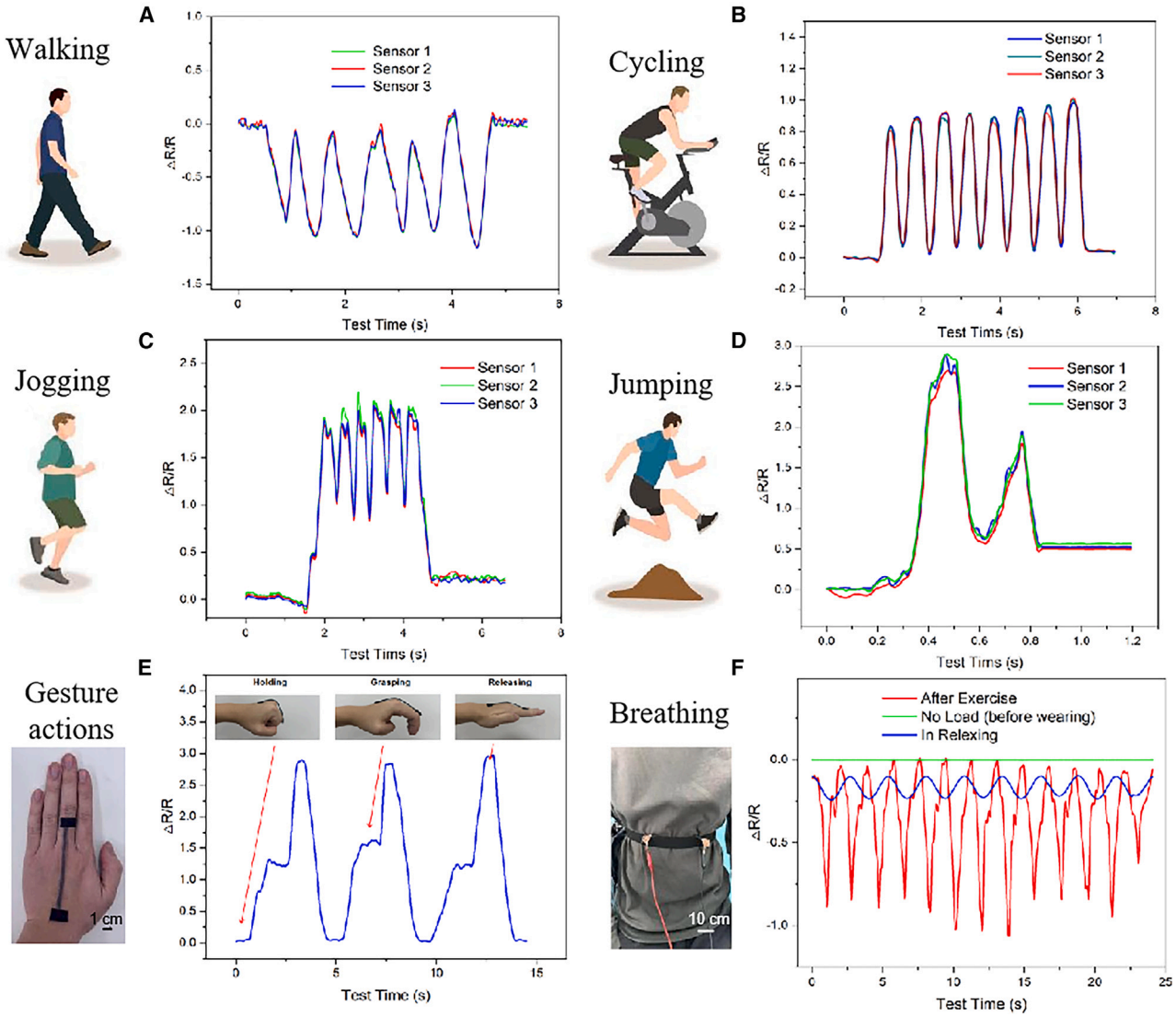

Figure 9. Wearable sensors applications

(A–D) Responsive curves of wearable sensor on the knee when, walking, cycling jogging, and jumping.

(E) Wearable sensor attached to the middle finger, detect different gesture motion.

(F) Responsive curves of wearable sensor on the wrist before wearing (no load), and under normal/exercise conditions.

RESOURCE AVAILABILITY

Lead contact

Further information and requests for resources and reagents should be directed to and will be fulfilled by the lead contact, Xuqing Liu (xqliu@nwpu.edu.cn).

Materials availability

This study did not generate new unique reagents.

Data and code availability

- All data reported in this paper will be shared by the lead contact upon request.
- This paper does not report original code.
- Any additional information required to reanalyze the data reported in this paper is available from the lead contact upon request.

ACKNOWLEDGMENTS

This work was financially support by the National Natural Science Foundation of China (52375204), Shaanxi Provincial Science and Technology Innovation Team under grant code 2024RS-CXTD-63, Xianyang2023 Key Research and Development Plan under grant code L2023-ZDYF-QYCX-009, and Shanghai Pujiang Program under grant code 23PJ1400700. I also wish to extend our heartfelt appreciation to my doctoral supervisor Dr Anura Fernando and Zhong Maiduo for graphic design work on this paper.

AUTHOR CONTRIBUTIONS

G.H. conceived the project and conducted the experiments. C.Z., Y.S., Y.Y., Y.W., and C.S. assisted in the experiments, analysis, and discussions of the results. C.Z., L.C., and X.L. supervised the project. All authors contributed to

the writing of the manuscript and gave approval to the final version of the manuscript.

DECLARATION OF INTERESTS

The authors declare no competing interests.

STAR★METHODS

Detailed methods are provided in the online version of this paper and include the following:

- KEY RESOURCES TABLE
- EXPERIMENTAL MODEL AND STUDY PARTICIPANT DETAILS
- METHOD DETAILS
  - Materials characterization
  - The harsh environment test
  - Sensing electro-mechanical test
  - Sensing performance of the graphene-coated cotton yarn
- QUANTIFICATION AND STATISTICAL ANALYSIS

SUPPLEMENTAL INFORMATION

Supplemental information can be found online at https://doi.org/10.1016/j.isci.2024.111711.

Received: August 12, 2024
Revised: September 10, 2024
Accepted: December 27, 2024
Published: December 30, 2024

REFERENCES

1. Weng, W., Chen, P., He, S., Sun, X., and Peng, H. (2016). Smart electronic textiles. Angew. Chem., Int. Ed. Engl. *55*, 6140–6169.
2. Wang, H., Zhang, Y., Liang, X., and Zhang, Y. (2021). Smart fibers and textiles for personal health management. ACS Nano *15*, 12497–12508.
3. Yao, S., Yang, J., Poblete, F.R., Hu, X., and Zhu, Y. (2019). Multifunctional electronic textiles using silver nanowire composites. ACS Appl. Mater. Interfaces *11*, 31028–31037.
4. Islam, M.R., Afroj, S., Beach, C., Islam, M.H., Parraman, C., Abdelkader, A., Casson, A.J., Novoselov, K.S., and Karim, N. (2022). Fully printed and multifunctional graphene-based wearable e-textiles for personalized healthcare applications. iScience *25*, 103945.
5. Kim, K.H., Jang, N.S., Ha, S.H., Cho, J.H., and Kim, J.M. (2018). Highly sensitive and stretchable resistive strain sensors based on microstructured metal nanowire/elastomer composite films. Small *14*, 1704232.
6. Lian, Y., Yu, H., Wang, M., Yang, X., Li, Z., Yang, F., Wang, Y., Tai, H., Liao, Y., Wu, J., et al. (2020). A multifunctional wearable E-textile via integrated nanowire-coated fabrics. J. Mater. Chem. C Mater. *8*, 8399–8409.
7. Daria, M., Krzysztof, L., and Jakub, M. (2020). Characteristics of biodegradable textiles used in environmental engineering: A comprehensive review. J. Clean. Prod. *268*, 122129.
8. Lu, Y., Jiang, S., and Huang, Y. (2010). Ultrasonic-assisted electroless deposition of Ag on PET fabric with low silver content for EMI shielding. Surf. Coating. Technol. *204*, 2829–2833.
9. Zhang, H. (2013). Silver plating on hollow glass microsphere and coating finishing of PET/cotton fabric. J. Ind. Textil. *42*, 283–296.
10. Xu, C., Zhou, R., Chen, H., Hou, X., Liu, G., and Liu, Y. (2014). Silver-coated glass fibers prepared by a simple electroless plating technique. J. Mater. Sci. Mater. Electron. *25*, 4638–4642.
11. Tao, Y., Han, F., Shi, C., Yang, R., Chen, Y., and Ren, Y. (2022). Liquid Metal-Based Flexible and Wearable Sensor for Functional Human–Machine Interface. Micromachines *13*, 1429.
12. Zhu, Z. (2017). An overview of carbon nanotubes and graphene for biosensing applications. Nano-Micro Lett. *9*, 25.
13. Robinson, J.P., Schomerus, H., Oroszlány, L., and Fal'ko, V.I. (2008). Adsorbate-limited conductivity of graphene. Phys. Rev. Lett. *101*, 196803.
14. Lee, H., Dellatore, S.M., Miller, W.M., and Messersmith, P.B. (2007). Mussel-inspired surface chemistry for multifunctional coatings. Science *318*, 426–430.
15. Kaminska, I., Das, M.R., Coffinier, Y., Niedziolka-Jonsson, J., Sobczak, J., Woisel, P., Lyskawa, J., Opallo, M., Boukherroub, R., and Szunerits, S. (2012). Reduction and functionalization of graphene oxide sheets using biomimetic dopamine derivatives in one step. ACS Appl. Mater. Interfaces *4*, 1016–1020.
16. Xie, L.-Q., Zhang, Y.-H., Gao, F., Wu, Q.-A., Xu, P.-Y., Wang, S.-S., Gao, N.-N., and Wang, Q.-X. (2017). A highly sensitive dopamine sensor based on a polyaniline/reduced graphene oxide/Nafion nanocomposite. Chin. Chem. Lett. *28*, 41–48.
17. Chen, Y., Zhang, Z., Huang, Z., and Zhang, H. (2017). Effects of oxygen-containing functional groups on the supercapacitor performance of incompletely reduced graphene oxides. Int. J. Hydrogen Energy *42*, 7186–7194.
18. Xie, Z., Yu, Z., Fan, W., Peng, G., and Qu, M. (2015). Effects of functional groups of graphene oxide on the electrochemical performance of lithium-ion batteries. RSC Adv. *5*, 90041–90048.
19. Zeng, L., Liu, X., Chen, X., and Soutis, C. (2018). Surface modification of aramid fibres with graphene oxide for interface improvement in composites. Appl. Compos. Mater. *25*, 843–852.
20. Nurazzi, N.M., Abdullah, N., Demon, S.Z.N., Halim, N.A., Azmi, A.F.M., Knight, V.F., and Mohamad, I.S. (2021). The frontiers of functionalized graphene-based nanocomposites as chemical sensors. Nanotechnol. Rev. *10*, 330–369.
21. García-Miranda Ferrari, A., Elbardisy, H.M., Silva, V., Belal, T.S., Talaat, W., Daabees, H.G., Banks, C.E., and Brownson, D.A.C. (2020). The influence of lateral flake size in graphene/graphite paste electrodes: an electroanalytical investigation. Anal. Methods *12*, 2133–2142.
22. Wu, S., He, Q., Tan, C., Wang, Y., and Zhang, H. (2013). Graphene-based electrochemical sensors. Small *9*, 1160–1172.
23. Liu, C., Hu, G., and Gao, H. (2012). Preparation of few-layer and single-layer graphene by exfoliation of expandable graphite in supercritical N, N-dimethylformamide. J. Supercrit. Fluids *63*, 99–104.
24. Zhang, Z., Huang, H., Yang, X., and Zang, L. (2011). Tailoring electronic properties of graphene by π–π stacking with aromatic molecules. J. Phys. Chem. Lett. *2*, 2897–2905.
25. Lee, J.H., Avsar, A., Jung, J., Tan, J.Y., Watanabe, K., Taniguchi, T., Natarajan, S., Eda, G., Adam, S., Castro Neto, A.H., and Özyilmaz, B. (2015). Van der Waals force: a dominant factor for reactivity of graphene. Nano Lett. *15*, 319–325.
26. Cheng, Y., Wang, R., Sun, J., and Gao, L. (2015). A stretchable and highly sensitive graphene-based fiber for sensing tensile strain, bending, and torsion. Adv. Mater. *27*, 7365–7371.
27. Wang, L., Liao, R., Tang, Z., Lei, Y., and Guo, B. (2011). Sodium deoxycholate functionalized graphene and its composites with polyvinyl alcohol. J. Phys. D Appl. Phys. *44*, 445302.
28. Afroj, S., Tan, S., Abdelkader, A.M., Novoselov, K.S., and Karim, N. (2020). Highly conductive, scalable, and machine washable graphene-based E-textiles for multifunctional wearable electronic applications. Adv. Funct. Mater. *30*, 2000293.
29. Arapov, K., Bex, G., Hendriks, R., Rubingh, E., Abbel, R., de With, G., and Friedrich, H. (2016). Conductivity Enhancement of Binder-Based Graphene Inks by Photonic Annealing and Subsequent Compression Rolling. Adv. Eng. Mater. *18*, 1234–1239.

STAR★METHODS

KEY RESOURCES TABLE

REAGENT or RESOURCE	SOURCE	IDENTIFIER
Chemicals, peptides, and recombinant proteins		
Deoxycholate(SDC)	Aladdin (Shanghai, China)	Cat#S274361;CAS no.302-95-4
Tris(hydroxymethyl)aminomethane	Meryer (Shanghai, China)	Cat#M26450; CAS no. 77-86-1
Dopamine hydrochloride	Aladdin (Shanghai, China)	Cat#D103111; CAS no. 62-31-7
Graphite	Asbury Graphite Mills, (USA,Asbury)	Cat#A60-1LB; CAS no.7782-42-5
Cotton Yarn	YaYing (Yiwu, China)	Cat#2.2-600
Nitrogen air	Makepolo (Zhengzhou, China)	CAS no.7727-37-9

EXPERIMENTAL MODEL AND STUDY PARTICIPANT DETAILS

Human participant : Gender:Male. Ancestry:Chinese. Race:Asian. Ethnicity:Chinese.

This study only involves one human participant, so there is a limitation for generalizability.

Sample size:10cm for the motion sensors on the knee angles and hand. 30 cm for the sensor beneath the chest.

The subjects/samples were randomly allocated to experimental groups.The subject of the experiment is the author of the article, and the subject consent to the use of the data.

METHOD DETAILS

Graphite , chosen for its smaller size (90% less than 30 micrometers), was used as the starting material to prevent clogging during the production process. Graphite flakes were combined with Sodium Deoxycholate (SDC) and mixed in deionized water (DI Water) to prepare the original graphite fluid. In the machine, the fluid was accelerated and circulated through microchambers with diameters less than 80 μm under 207 MPa pressure, achieving exfoliation. Each passage through the microchamber is considered one cycle. The Schematic diagram of micro fluidization process is presented in Figure S10. Here, the Graphene dispersion solution were synthesized by a mixture comprising 10 grams of graphite, 1 gram of sodium deoxycholate (SDC), and 50 milliliters of deionized water was prepared and processed through a microfluidizer for 100 cycles.

Dopamine was dissolved in a 0.01 mol L^{-1} tris (hydroxymethyl) aminomethane buffer (pH 8.5) at a concentration of 2 g L^{-1}. Cleaned cotton yarns were then immersed in this solution. Stirring and vertical sample orientation were utilized to prevent nonspecific microparticle deposition on the surfaces. The pH-induced oxidation of dopamine turned the solution dark brown. After 24 hours, the resulting polydopamine (PDA) film-coated surfaces were filtered, thoroughly rinsed with DI water, and dried using a N_2 gas stream. The PDA-modified yarn was dip-coated into the graphene dispersion solution for via self-made coating system then dried at an air cabinet for 24 hours. This coating process was repeated twice to produce conductive yarns with relatively low electrical resistance, suitable for wearable sensors used in e-textiles and beyond.

Materials characterization

The lateral size and thickness distribution of graphene dispersion was characterized with a Field emission scanning electron microscopy (SEM, CLARA GHM) and Atomic Force Microscope (AFM, MultiMode 8). The raman spectrum was collected by the Horiba LabRAM HR Evolution with an 532nm wavelength. The poly-dopamine modified sensor yarn was identified with Fourier Transform Infrared Spectroscopy (FTIR, IR Tracer-100). X-ray photoelectron spectroscopy was collected by the PHI5000. The mechanical tests of sensor were undergoing by the Zhiqu tensile test machine and the resistance was measured by the KEITHLEY 2611B Source Measure Units.

The harsh environment test

The UV chamber(Cheng Ju Instrument Co., Ltd., Suzhou) is shown by Figure S3. The test samples, both modified and unmodified yarns, were cut to 10 cm and coated with graphene using the 2-cycles dip-coating method before being weighed to record the amount of graphene adsorbed on the yarn prior to the experiment. The temperature inside the chamber risen to about 65°C and remain stable after device turn on. The tested yarns were affixed to white paper with double-sided 3M adhesive tape, and a 100g weight was placed on an acrylic panel to apply even pressure to the yarns, ensuring firm adhesion to the 3M tape. After waiting for one hour, the samples were removed, the test yarns were peeled off, and weighed the weight loss.

Sensing electro-mechanical test

Figure S8 shows the sensing electro-mechanical test tests. The cyclic bending tests was present by Figure S8A. Sensors were cut into 10 cm long samples and secured at both ends by grips. To ensure uniform bending, a strip of paper was attached to the back of the sensor, and copper foil were used at both ends to ensure the clips could grip the sensor ends securely. As the gauge Length was reduced, the paper strip bent uniformly, driving the bending of the sensor and recording the resistance readings. Figure S8B shows the sensor tensile test. Similar to the cyclic bending tests, the sensors were cut into 10 cm long samples and fixed at both ends by grips, and stretched at a rate of 2 mm/s. The resistance and stress of the sensor were recorded, and the test was interrupted when the stress reached 20% of its maximum value. Figure S8C illustrates the sensor's lateral compression test. Sensors were cut into 10 cm lengths and attached to alligator clips at both ends for resistance testing. To prevent interference from the metal substrate on the resistance, insulating fabric was placed under the sensor, and pressure was applied to the sensor through a 1 cm x 1 cm sized block press. The stress was calculated based on the Load/Area applied by the press.

Sensing performance of the graphene-coated cotton yarn

The electro-mechanical properties of the graphene-coated cotton yarn sensors were evaluated using a ZQ-990L computerized tensile testing machine (Zhiqu Instrument Co., Ltd., China). In this setup, the cotton yarn sensors were placed between two compression plates of the tensile machine. The upper plate was moved downward at a controlled speed of 2 mm/min, while the lower plate remained stationary (as illustrated in Figure S10). The sensitivity (S) of the piezoresistive sensor, a critical parameter for assessing device performance, was calculated using the following equation:

$$S = \frac{\Delta R}{R_0} \times 100\% = \frac{R - R_0}{R_0} \times 100\%$$

where ΔR denote the resistance change before and after load applied, R and R_0 denotes the deformed and undeformed samples' resistances, respectively. To further investigate the sensor's performance, cord lengths were used during bending tests to measure resistance changes. The sensor's cord length was adjusted by move the distance between the two grips of the tensile machine. The certain length of the graphene-coated cotton yarn sensors were placed on the joint and lower chest location of participants for the movement and respiratory signal capturing. The sensor's resistance changes during tensile testing, bending tests, joint movement tests, and respiration monitoring were recorded using a KEITHLEY 2611B Source Measure Unit.

QUANTIFICATION AND STATISTICAL ANALYSIS

Figures represent averaged or representative results of multiple independent experiments. Analyses and plots were performed with Origin.